



Observed turbulence characteristics in unstable conditions over the city of Tehran based on similarity theory

N. Pegahfar¹ · P. Zawar-Reza²

Received: 26 January 2016 / Accepted: 27 September 2016 / Published online: 19 October 2016
© Springer-Verlag Wien 2016

Abstract In a previous study, applicability of Monin–Obukhov similarity theory (MOST) was established for stable and relatively neutral conditions for Tehran, based on local scaling approach. This paper extends the application of MOST to unstable conditions for Tehran using SODAR data and five 2-D sonic anemometers. Normalized standard deviations of three components of wind velocity ($\sigma_{u,v,w}/u_*$, u_* is friction velocity) as functions of $\zeta = (z - z_d)/\Lambda$ stability parameter (where Λ is the local Obukhov length, z is the height of measurement and z_d is the zero-plane displacement height) have been computed and analyzed at various levels. Only the parameters measured at 105 m height provided sufficient accuracy for MOST evaluation and also reliable universal similarity relations, while those at the lower heights (45 and 75 m) did not match MOST. Near zero dependence of σ_w/u_* on ζ motivated further investigation using convective velocity scale and also another stability parameter (defined using mixed-layer height). Applying the second scaling parameters leads to more suitable similarity functions. For the present research, we demonstrate that under unstable conditions, normalized values of $\sigma_{u,v,w}$ could be collapsed into the similarity expressions, but are highly dependent on proper

selection of scale and vertical position. So for the case of Tehran, transformation from one kind of similarity scale to another one is possible, as suggested by Hu and Zhang (Sci Atmos Sin 17:10–20, 1993), with the provision that it only works for certain focused variables and vertical position. In addition, we show significant differences in empirical constants between Tehran and the values reported for the other cities in the literature (from the other surface types). This is most likely due to the local effects of the underlying surface (both urban area and topographical features) in Tehran.

1 Introduction

Despite its semi-empirical nature, Monin–Obukhov similarity theory (MOST) is widely used to describe the structure and characteristics of turbulence in the surface layer through scaling parameters derived from dimensionless ratios (Monin and Obukhov 1954). MOST has its own set of advantages and disadvantages (Adrian 2002) and was developed strictly for homogenous surfaces over the flat terrain of Kansas (Wyngaard and Cote 1971). As stated by Wilson (2008); “parsimony, accessibility and convenience” makes MOST an appealing tool for boundary-layer research. Numerous scientists have tried to apply this theory in conditions that deviate from its basic assumptions, for example Grachev et al. (2005) applied MOST for stable stratification, Roth et al. (2006) and Mahrt (1998b) under unstable stratification, Yusup and Lim (2012) for a complex terrain, Martins et al. (2009) for heterogeneous landscapes, Anfossi et al. (2005) for the flat urban area of Graz in Austria, and Hagishima et al. (2009) for wind tunnel data. Also MOST validation was conducted for

Responsible Editor: S. T. Castelli.

✉ N. Pegahfar
pegahfar@inio.ac.ir

P. Zawar-Reza
peyman.zawar-reza@canterbury.ac.nz

¹ Atmospheric Sciences Research Center, Iranian National Institute for Oceanography and Atmospheric Science, Tehran, Iran

² Department of Geography, University of Canterbury, Christchurch, New Zealand

various surface types in different climate regimes, for example in rural areas (Nieuwstadt 1984), over Arctic pack ice (Grachev et al. 2007a), over a salt lake (Princevac and Venkatram 2007), in a forested area (Moraes et al. 2005), in a sub-urban area (Mortarini et al. 2009) and in several urban areas in different climatic settings (Rotach 1993a, b) in Zürich; Al-Jiboori 2008 in Beijing; Hanna et al. 2007 in Oklahoma City and Manhattan).

It is obvious that MOST is also the most common method applied to the surface layer in Numerical Weather Prediction (NWP) models (Bou-Zeid et al. 2009; Castillo et al. 2011; Inagaki and Kanda 2010). In spite of MOST's underlying assumptions, many researchers have tried to evaluate this theory to atmospheric conditions associated with significant horizontal and vertical advection (Katul et al. 1995), significant surface heterogeneity (Lamaud and Irvine 2006), unsteady conditions (McNaughton and Laubach 1998), significant mesoscale effects (Asanuma and Brutsaert 1999), gravity or canopy waves (Finnigan et al. 1984; Cava et al. 2004), and low-level jets (Prabha et al. 2007). Also Pegahfar and Bidokhti (2013), hereafter PB13, have previously validated MOST for Tehran under stable and relatively neutral stratifications (based on local scaling approach). They concluded that this theory produced reliable prediction of non-dimensional parameters at 105 m height, which is well above the roughness sub-layer. Also they showed that similarity theory is violated under stable stratification at the lower heights (45 and 75 m) over Tehran.

It is obvious that knowledge of turbulence characteristics under various conditions is needed for evaluation of numerical simulations especially for complex terrain. Hence to provide enough knowledge for further research, we extend the previous work done by PB13 and investigate the applicability of MOST under unstable stratification over Tehran in this paper. To achieve this, we employ two groups of scales from inner- and outer-layer in the current research and structured this paper as follows: after describing the experimental site and its surface-layer climatology (Sect. 2), instrumentation and data are introduced (Sect. 3), followed by methods in Sect. 4. The results of MOST validation, using two groups of scales are discussed in Sect. 5. The conclusion in the last section highlights whether or not this theory is applicable under unstable stratification for Tehran.

2 Experimental site and surface-layer climatology

Tehran area and the selected station have been shown in Fig. 1 (more detailed characteristics have been presented by PB13 and Pegahfar et al. 2011). The northern mountains range perturbs the low-level wind over Tehran by

generating thermally forced mesoscale flows (Pegahfar et al. 2011), in addition to the heat island effect which modifies Tehran boundary-layer (Zawar-Reza et al. 2010; Pegahfar et al. 2011). The vertical profiles of horizontal components of wind velocity over Tehran have been shown to be complex and exhibit directional shear (Fig. 2). Moreover, Tehran exhibits complex profiles of daily averaged sensible heat flux ($\overline{\theta'w'}$), calculated using gradient relation. Values of $(\overline{\theta'w'})_{(2-10m)}$ and $(\overline{\theta'w'})_{(45-100m)}$, show its strongly height dependency (Fig. 3). Since the maximum and minimum values of sensible heat flux occurred in January and July, only results have been shown for these months. It is worthwhile to note the positive averaged nocturnal values of $\overline{\theta'w'}$ even for the upper layer (45–100 m). Also, this area experienced the calculated storage term, as the ratio of sensible heat flux from two levels (Moriwaki et al. 2002), with the values smaller than 0.3 for $z/L < -0.1$ (Pegahfar et al. 2011). Here, L is the Obukhov length. The other characteristics of Tehran such as height dependent heat flux, the height of surface layer, and also non-isotropic flow have been shown by Pegahfar et al. (2011) and PB13. Overall, it can be assumed that the height of 105 m lies in the surface layer, based on (a) PB13 findings through the characteristics of turbulent structure under stable stratification, (b) assuming surface layer to be the lowest 10 % of mixed-layer height which was shown to be around 3 km over Tehran (Ahmadi-Givi et al. 2008), and (c) horizontal wind velocity profiles provided by Pegahfar et al. (2011) (their Figs. 3–6).

3 Instrumentation and data

Instruments employed for this research are located at the Institute of Geophysics at the University of Tehran located less than 5 km away from the southern foothills of the Alborz Mountain chain. For the presented analysis, three datasets have been used as itemized below:

1. The main instrument is a PA1 SODAR (at $35^{\circ}44'48.2''N$ and $51^{\circ}23'11.8''E$), described by PB13. SODAR setup with typical operating parameters including up to 20 range gates, with typical spacing of 10–200 m, and averaging times from 2 min to 1 h. Also the beam tilt was set to 30° or 15° , based on the recommendation in the technical manual. Vertical and horizontal speed accuracy is ± 15 and ± 20 cm/s, respectively. We used continuous quality controlled measurements from January to August 2007.
2. To verify and compliment the SODAR measurements, data from a 100-m tower ($35^{\circ}44'25.6''N$ and $51^{\circ}23'11.0''E$) that is approximately 150 m away from DODAR station have been used. The tower is equipped

Fig. 1 The studied area, including a map of Tehran topography and its surrounding region using Origin Lab software in (a) and Google Earth software in (b). The star and place mark indicate the location of Geophysics station in the Institute of Geophysics at the University of Tehran

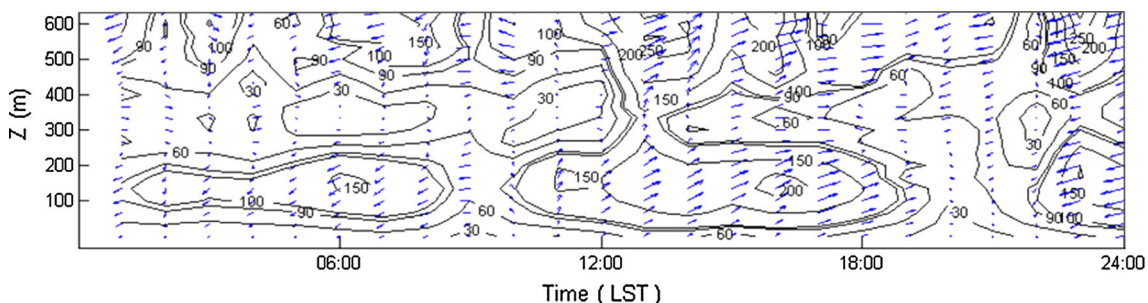
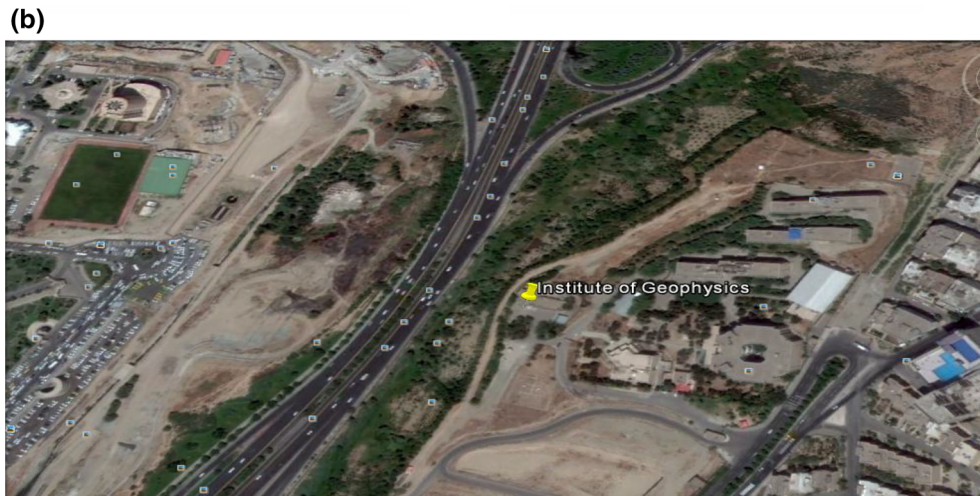
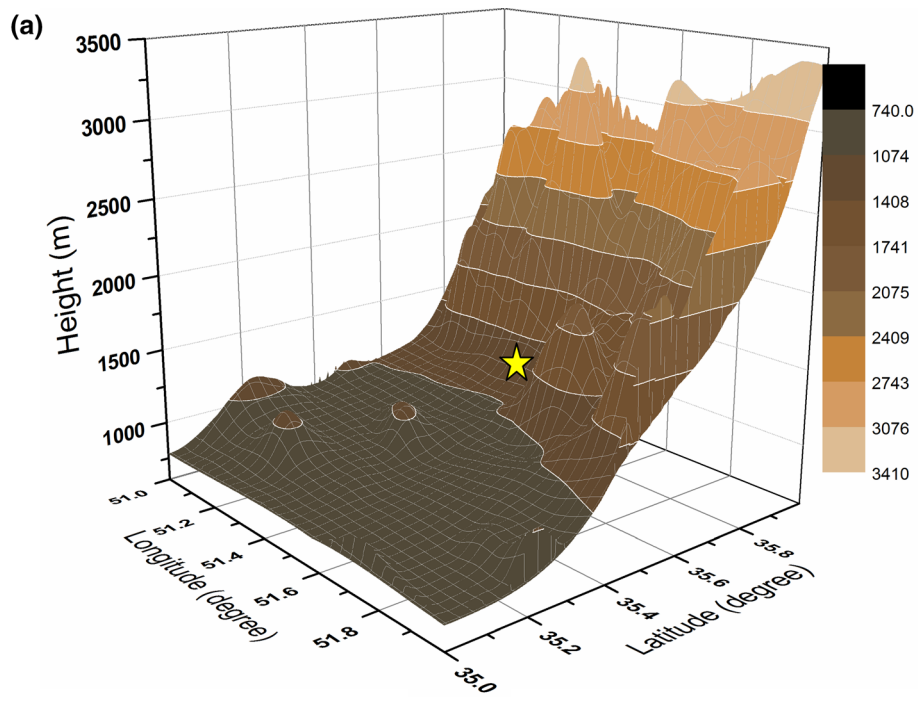


Fig. 2 Monthly averaged values of hourly SODAR wind (u, v) profile (cm/s) and wind speed contour for March 2006 15–585 m height with 30 m vertical resolution. The blue arrows show horizontal

wind velocity and solid contours indicating wind speed with 30 cm/s intervals for $U < 100$ cm/s and 50 cm/s intervals for $U > 100$ cm/s (captured Pegahfar et al. 2011)

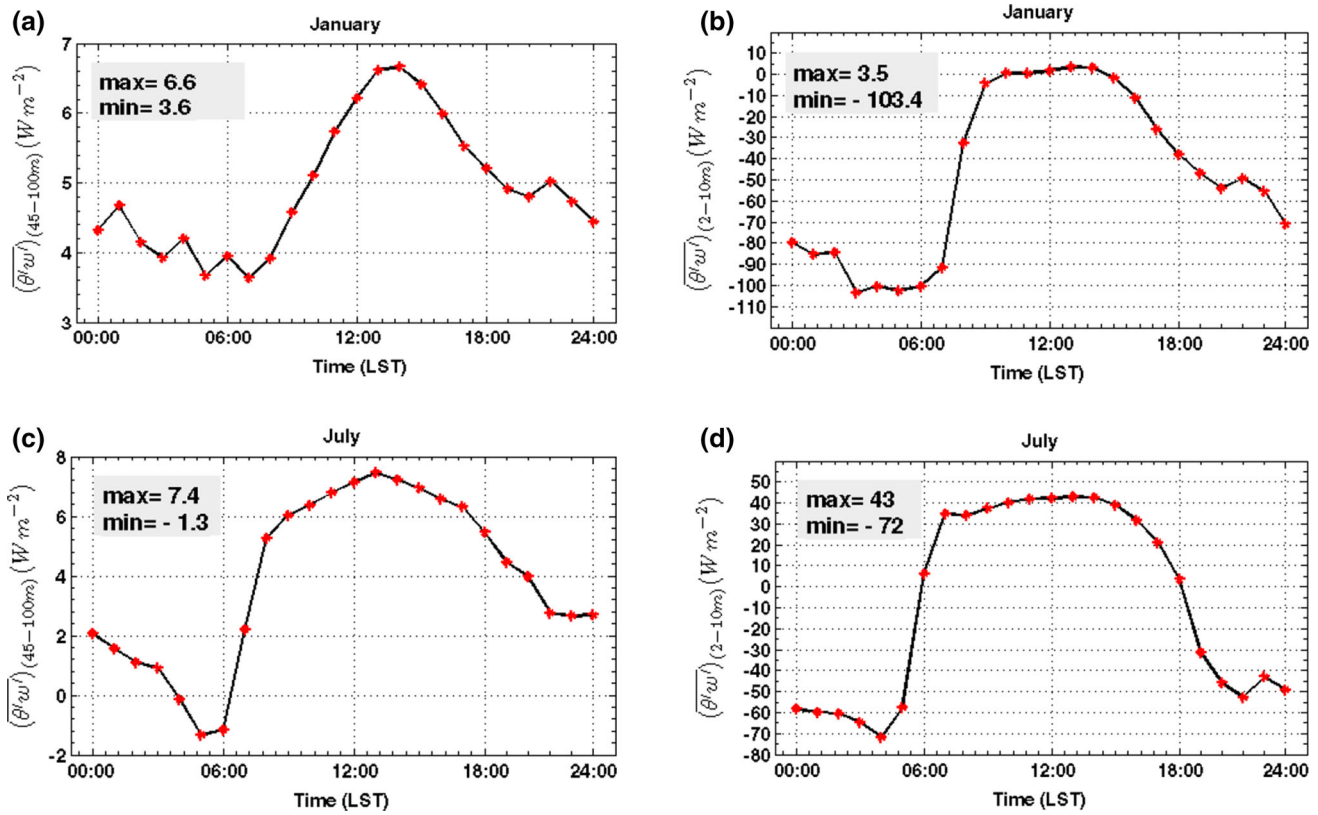


Fig. 3 Monthly averaged values of hourly sensible heat flux for January (top panels) and July (lower panels), based on gradient relation. The results of using data measured at 45 and 100 m levels have been shown in the left column, while the results of using the data measured at the levels of 2 and 10 m have been depicted in the right

column. All panels have been plotted using data measured by the sonic anemometers installed on the tower. The left column has been taken from Pegahfar et al. (2011) and modified for the current work, while the right column has been 736 only discussed by them

with four 2-D sonic anemometers, installed at 2, 10, 45 and 100 m heights. More detailed characteristics have been reported by PB13.

3. To compute the mixed-layer height according to the peak frequency of the spectra of u - and v -components of wind velocity, data measured by a 2-D sonic anemometer (installed at 2 m height) located at SODAR station were also used. Data were acquired at 10 Hz and included u , v and T variables. Comparing with the lowest height of SODAR data as 15 m, the height of measured data by the above 2D sonic anemometer as 2 m is more close to the height of 2.9 m used in the defined technique for mixed-layer determination by Liu and Ohtaki (1997) and Murty et al. (1998), more details have been presented in Sect. 4.

4 Methods

Before proceeding the validation of MOST, necessary constraints were applied to the dataset as explained in this section. Subsequently, we present the employed formulations

together with the pertinent characteristics of the derived parameters.

4.1 Data processing

It is well-known that SODARs have some limitations which depending on the environmental conditions may affect the quality of data. These include attenuation of the acoustic waves, volume sampling, spatial and temporal separation of sampling volume, slow speed of sound, and assumption of constant tilt for the electronically steered beam. There is strong evidence that SODAR measurements can provide comparable data to instruments that sample from a point (Ito 1997; Thomas and Vogt 1993; Melas 1991; Garratt 1982; Seibert and Langer 1996). SODAR measurements have also been verified in complex terrain, for example, Petenko et al. (2012) used SODAR data in the vicinity of the European Alps and demonstrated the accuracy of the method. Also, PB13 checked u , v and T trends and reached a good consistency between data measured by SODAR and other instruments despite being 150 m apart horizontally. In the current research to ensure quality, we

examined SODAR-driven horizontal wind and their fluctuations at various heights. For an example, results derived at 45 m height are presented below.

The 30-min averaged values of u - and v -components of wind at 45 m height measured by the sonic anemometer, installed at 45-m height on the tower, were plotted against those measured by SODAR (Fig. 4a, b). The obtained correlation equation for along-wind component was $u_{\text{sonic anemometer}} = 1.287u_{\text{SODAR}} - 0.350$ and for cross-wind one was $v_{\text{sonic anemometer}} = 1.067v_{\text{SODAR}} + 0.134$. Their related correlation coefficients ($R = 0.91$ and 0.86 for u - and v - components of wind, respectively) showed reasonable agreement between SODAR and sonic anemometer data, same as Ito (1997) results with $R = 0.96$. Moreover, the correlation of σ_u and σ_v data (standard deviations of horizontal components of wind) between the sonic anemometer and SODAR measurements (both at 45 m height) were investigated (Fig. 4c, d). The correlation equations for σ_u and σ_v were $\sigma_{u_{\text{sonic anemometer}}} = 0.815\sigma_{u_{\text{SODAR}}} + 0.107$ and $\sigma_{v_{\text{sonic anemometer}}} = 0.983\sigma_{v_{\text{SODAR}}} - 0.059$ in that order. It is noticeable that our gained correlation coefficient for σ_v ($R = 0.84$) was bit larger than that for σ_u ($R = 0.82$), similar to Ito (1997) findings. In addition, it can be assumed that σ_u and σ_v values from SODAR and the sonic anemometer had well correlation, considering

Gaynor and Kristensen (1986) results which showed that these parameters had no bias under convective cases. Since no vertical component of wind have been measured by the tower-sonic anemometers, so we assume that σ_w from SODAR had an acceptable bias, based on Kouznetsov et al. (2007) results. Also comparison of temperature values measured by the 2 m height sonic anemometer located at SODAR station and the 2 m height sonic anemometer installed on the tower showed well agreement.

Following, to satisfy assumptions of MOST, a few constraints were imposed to minimize probable uncertainties from environmental conditions in our SODAR data that outlined below as: (a) the first eight constraints explained by PB13, (b) to ensure stationarity, the method proposed by Mahrt (1998a) has been followed (listed in Table 1). In the current work, 30-min periods have been selected that each period includes 5 records ($i = 1, 5$) and each record contains six 1-min segments ($j = 1, 6$). The non-stationary ratio (NR) is unity for stationary conditions, for our dataset any value above 0.8 has been considered to exhibit stationarity (for more details see PB13, second paragraph in Sect. 2.2.1). It is important to note that after processing the data, we are confident that, inaccuracies due to environmental condition on SODAR measurement have been minimized. These errors may occur because of basis

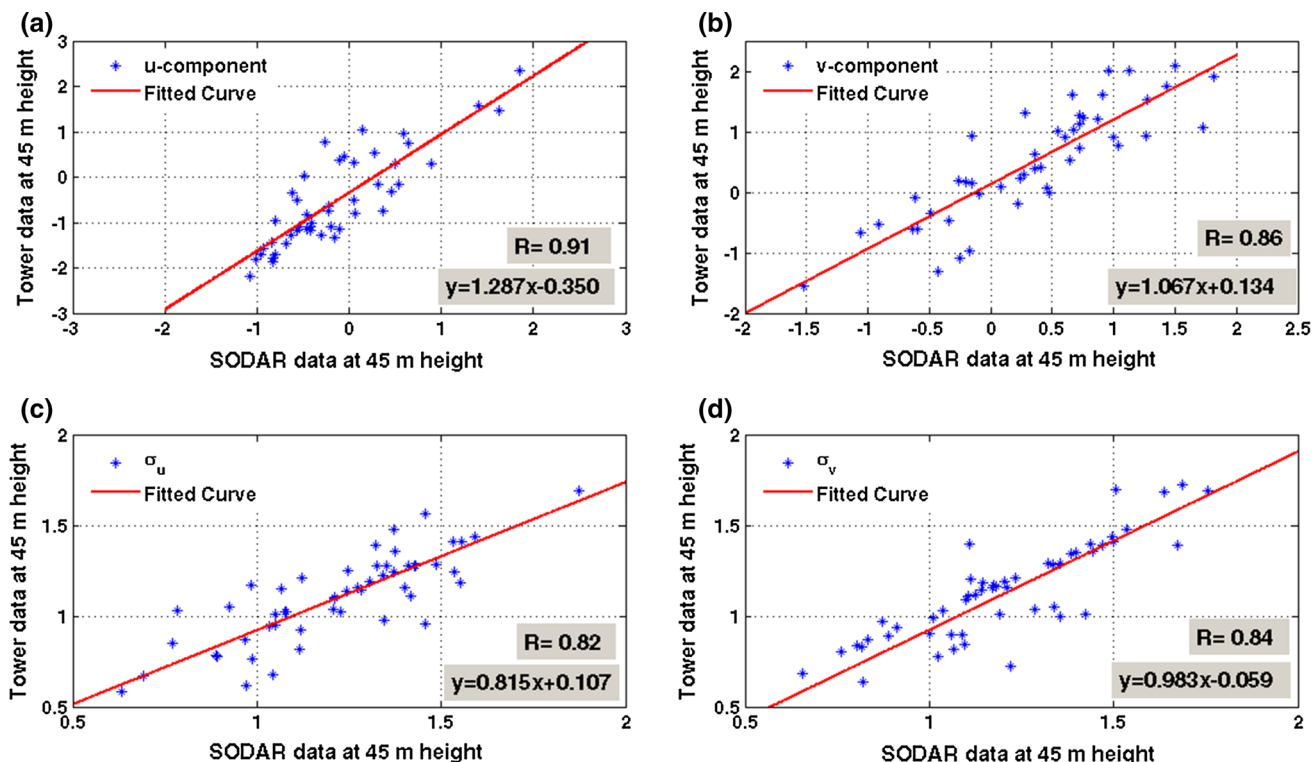


Fig. 4 Scatter diagram of data measured by sonic anemometer against those measured by SODAR, both at 45 m height, for u -component of wind (a), v -component of wind (b), σ_u (c) and σ_v (d).

The *fitted line* and its equation are shown in each subplot. The number of data is between 40 and 50

Table 1 Utilized formula to calculate non-stationary ratio during 30-min periods. Each period contains five records ($i = 1, 5$) and each record contains six 1-min segments ($j = 1, 6$)

Num.	Relation	Definition	Comment
1	$\sigma_{wi}(i) = \sqrt{\frac{1}{J-1} \sum_{j=1}^J [F(i,j) - \bar{F}(i)]^2}$	Standard deviation within records	J is number of the segment $F(i,j)$ is the flux of some arbitrary quantity for j th segment of i th record \bar{F} is the average of these segment fluxes for i th record σ_{wi} is standard deviation within a record
2	$RE = \frac{\sigma_{wi}}{\sqrt{J}}$	Standard deviation within a record	RE is random error
3	$\sigma_{btw} = \sqrt{\frac{1}{I-1} \sum_{i=1}^I [\bar{F}(i) - \bar{F}]^2}$	Standard deviation between records	I is number of the record \bar{F} is the average of flux over all of segments and records $\bar{F}(i)$ denotes the average of the flux for j th record σ_{btw} is standard deviation between records
4	$NR = \frac{\sigma_{btw}}{RE}$	Nonstationary ratio	

that with our reasons for their ignorable influences have been itemized as below:

1. Volume averaging, the data strictly speaking are not the same as point measurements obtained by the tower instruments, however, reasonable agreements have been achieved in the current work similar to results of Petenko et al. (2012) and Melas (1991) as both datasets are comparable;
2. Shear effect, but this was shown to be insignificant for unstable stratifications at 105 m height (well away from the roughness sublayer), because we are only using periods with small values of up- and downdraft (of $-80 < w$ (cm/s) < 115), see also Seibert and Langer (1996);
3. Beam tilt, but this is also insignificant because of small variation of temperature ($0.3 < |T_{100m} - T_{45m}| < 1.6$) and $U < 5$ m/s.

4.2 Local Obukhov length (Λ)

The local Obukhov length has been calculated based on the relation of $\Lambda = -u_{*,l}^3 \bar{T} / kgw'\bar{T}'$. Here, u_* is friction velocity calculated using the relation of $u_{*,l} = [\overline{u'w'}^2 + \overline{u'w'}^2]^{1/4}$ and momentum fluxes from SODAR data, whereas T (K), $w'\bar{T}'$ (K m/s), k and g (m/s) denote temperature, heat flux calculated based on gradient relation, Von-Karman constant and gravity acceleration, respectively, while “ l ” subscribe shows local value and over bar represents averaged value (Table 2, rows 1 and 2). The range of negative local Obukhov length, calculated at 105 m height, has been shown in Fig. 5. The low frequency of neutral condition indicates that turbulence in outer-layer contains energetic

eddies and is highly convective. So turbulence in this layer is significant over Tehran, based on Laubach and McNaughton (2009) results. They showed that neutral conditions could be characterized by (a) weak outer convection, (b) strong surface shear, (c) less energetic outer eddies, and (d) more energetic inner eddies. Also the low frequency of neutral conditions for Tehran could be due to the large coherent structures found in urban turbulence due to the special terrain as proved by Feigenwinter and Vogt (2005) for roughness effect.

4.3 Stability parameter (ζ)

The derived ζ values for Tehran show a wide range of stability conditions (from PB13). Since the number of daily and nocturnal measurements is approximately equal, it can be inferred that unstable stratification is dominant in this area even at night. That maybe the result of positive contribution of buoyancy term during the nighttime hours (see Fig. 12 from Pegahfar et al. 2011), thought be caused by the release of stored heat from the urban canopy (Nakamura and Oke 1988; Weber and Kordowski 2010) or anthropogenic heat flux and radiative trapping (Christen and Vogt 2004).

In the current work, using the limit proposed by others to distinguish unstable from neutral cases led to inaccurate results, because of lack of data around the suggested values (e.g. $\zeta = -0.02$ suggested by Moriawaki and Kanda 2006, $\zeta = -0.1$ used by Christen 2005 and $\zeta = -0.05$ employed by Inagaki and Kanda 2008; Dettò et al. 2010; Castillo et al. 2011; Feigenwinter et al. 1999). To solve this problem, we used another scale ($\mu = h/\Lambda$; Table 2), based on local Obukhov length (Λ) and boundary-layer height

Table 2 List of calculated variables and related relationships

Num.	Variable	Formula	References	The uncertainty in the present paper	Data and description
1	Velocity scaling (m/s)	$u_* = [u'w'^2 + v'w'^2]^{1/4}$	Britten and Hanna (2003)	±0.1	SODAR $u'w'$ is streamwise momentum flux $v'w'$ is spanwise momentum flux
2	Length scaling, local Obukhov length (m)	$\Lambda = -u_{*l}^3 \bar{T} / kgw\bar{T}'$	Neuwstadt (1984)	±0.04	SODAR Tower sonic anemometers u_* (m/s), T (K), $w' T'$ (K m/s), k and g (m s ⁻²) denote friction velocity, temperature, heat flux, Von-Karman constant and gravity acceleration, respectively
3	Stability parameter	$\zeta = (z - z_d)/\Lambda$		±0.02	l is local value SODAR Tower sonic anemometers
4	Normalized planetary boundary layer height	$\mu = h/\Lambda,$ $h = cu_*/ f_{co} $	Cvitan (2006), Arya (1981) with $c = 0.4$ for unstable conditions	±0.07	z (m) and z_d (m) show height of measurement, zeroplane displacement height, respectively SODAR Tower sonic anemometers Sonic anemometer at SODAR location
5	Normalized standard deviation	$\varphi_i = \frac{\sigma_i}{u_{*i}},$ $i = u, v$ and w		Less than ±0.05	h (m), c and f_{co} (rad/s) is boundary layer height, constant and coriolis parameter, respectively SODAR σ_i (m/s) is standard deviation for i th component of wind velocity
6	Convective velocity scale	$w_*^3 = (g/T)(w'T)_0 Z_i$		±0.09	SODAR Tower sonic anemometers Sonic anemometer at SODAR location
7	Mixed-layer height (m)	$z_i = 0.8\bar{U}/f_{max}^u,$ $z_i = 0.75\bar{U}/f_{max}^v$	Murty et al. (1998), Liu and Ohtaki (1997)	±1.3	Z_i (m) and 0 denotes Mixed layer height and surface measuring, respectively Sonic anemometer at SODAR location f_{max}^u and U (m/s) shows maximum peak frequency in the spectra of horizontal wind velocity components and wind velocity, respectively

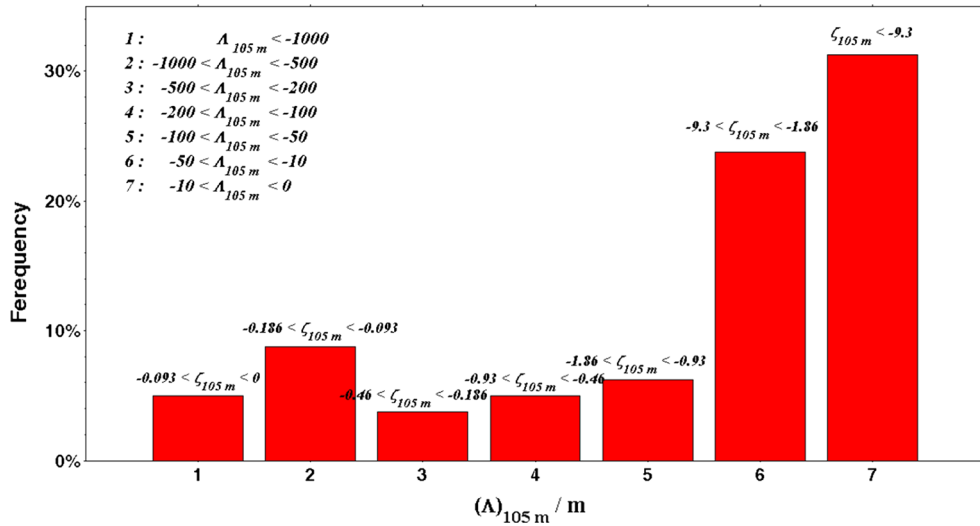


Fig. 5 Frequencies of local Obukhov length values calculated based on variables measured at 105 m height under unstable stratification ($\Lambda_{105\text{m}} < 0$) using original dataset before implementing constraints. For this aim, SODAR measurements at 105 m height were used. Also the heat flux values have been linearly extrapolated at 105 m height using the related values from the lower levels measured at 100-m

tower. Extrapolation has been done applying Matlab' curve fitting toolbox. Each number in abscissa belongs to one category defined in the *upper part* of the plot. In addition, limits of stability parameter $\zeta_{105\text{m}} = \left[\frac{\bar{z}(=105) - z_d}{\Lambda_{105\text{m}}} \right] < 0$ are included at the top of each bar

(*h*) containing mixed-layer height and clouds (sometimes), see Fig. 1.7 from Stull (1988) for more details. The stability parameter μ , introduced by Cvitan (2006), is more appealing because it is less dependent on u_* . Following, the current dataset in the unstable conditions has been subcategorized into two classes of unstable ($-10 > \mu$) and slightly unstable ($-10 < \mu < 0$) stratifications. There is a degree of overlap for Λ values in both μ stability classes, as well as for ζ values. The sharp variation of normalized parameters when ζ approaches zero (toward neutral stratification) led us to set the initial boundary of the unstable condition to $\zeta = -1$. In addition, MOST was applied only to the unstable cases here, because the normalized standard deviations of wind velocity components under slightly unstable condition were close to the values for the slightly stable condition as reported by PB13. Also the extremely unstable conditions have not been examined, because (a) the implementation of the constraints (for more details see Sect. 2.1.1 in PB13) severely reduces the size of dataset, making it unsuitable for analysis and (b) surface-layer similarity theory reaches its limits of applicability under extremely unstable conditions—the so-called free convective regime (Pahlöw et al. 2001).

4.4 Mixed-layer height (z_i)

In the current work, the mixed-layer height values were calculated using the method defined by Liu and Ohtaki (1997) and Murty et al. (1998). For this aim, data measured

by the sonic anemometer located at SODAR station were binned in 2-hourly intervals, and power spectral density $S(f)$ (f Hz) is the frequency and S (W/Hz) is the spectrum energy density) were calculated for the spectra of u - and v -components of wind velocity. After calculating the peak frequency (f_{\max}), the mixed-layer depth was computed by arithmetic mean of the calculated values of z_i from u and v spectra for each 2-h bin (Table 2, 7th row). For the u spectrum, coefficient of 0.8 as suggested by Murty et al. (1998) was applied. This procedure results in a computed height of 3 km for mixed layer, consistent with the finding by Ahmadi-Givi et al. (2008).

5 Results and discussion

In this section, the results of validation of similarity theory for unstable conditions are presented for two groups of scales, using different velocity and length scales. The selected scales in the first group are u_* friction velocity and Λ local Obukhov length, and those in the second group are w_* convective velocity and z_i mixed-layer height. It is notable that determination coefficients in fitting curves for φ_i against ζ values at 45 and 75 m heights were very small (Table 3, the first and second rows) and figures have not been shown. So it was concluded that similarity theory could not be applied for the levels lower than 105 m height under unstable condition, similar to the results obtained by PB13 for stable condition.

Table 3 Our derived empirical constants of a_i , b_i and c_i (according to Eq. 1), before and after self-correlation correction at 45, 75 and 105 m heights, together with an overview of constants in the earlier published empirical fits

No.	Authors and descriptions	- $[z - z_d]/\lambda > 0$, Constant						σ_w/u_{*i}	
		σ_u/u_{*i}			σ_v/u_{*i}				
		a_u	b_u	c_u	a_v	b_v	c_v		
1	Present work, urban area with complex topography, Tehran							$R^2 = 0.088$	$R^2 = 0.079$
	a. At 45 m height							$R^2 = 0.29$	$R^2 = 0.32$
	b. At 75 m height							$R^2 = 0.28$	$R^2 = 0.32$
	c. At 105 m height, after self-correlation correction	3.234	0.267	—	3.424	0.146	—	2.38	0.0051
	d. At 105 m height, before self-correlation correction	2.69	0.62	—	2.8	0.37	—	2.38	0.0051
2	Xu et al. (1997)	Campus of Nanjing University near the city centre	2.30	2.01	—	2.10	1.77	—	1.35
3	Roth (2000)	A review for some cities	1.98	0.33	0.56	2.8	0.37	2.8	1.12
4	Al-Jiboori et al. (2002)	Beijing City	1.75	1.80	—	1.6	2.10	—	1.22
5	Krishnan and Kunhikrishnan (2002)	Semi-arid region in Ahmedabad	None	None	None	None	None	None	1.05
6	Quan and Hu (2009)	325-m meteorological tower in Beijing	2.03	0.5	—	1.70	1.05	—	1.33
7	Wood et al. (2010)	At height 190.3 m on a telecommunications tower in west-central London	2.23	0.22	—	1.78	0.57	—	1.31
8	Weber and Kordowski (2010)	Urban site, Essen, Germany	1.98	0.53	0.57	2.03	0.32	0.86	1.22
		Urban park, Essen, Germany	1.93	1.28	—	1.96	1.37	—	1.29
									0.62

If constant c is not explicitly given in the table, it was set to 0.33. Both approaches (constant c , variable c) provided for comparison purpose. All of the empirical constants for the present work have been achieved using Matlab® Curve Fitting Toolbox with 95 % confidence bounds

5.1 Normalized fluctuations of wind velocity components, using u_* and Λ scales

Dependence of dimensionless standard deviations for three components of wind velocity (σ_i/u_* , $i = u, v, w$) as a function of $(z - z_d)/\Lambda$ has been investigated according to:

$$\varphi_i \left(\frac{z - z_d}{\Lambda} \right) = \left(\frac{\sigma_i}{u_*} \right) = a_i \left(1 + b_i \left(\frac{z - z_d}{\Lambda} \right) \right)^{c_i}, \quad (1)$$

$i = u, v, w.$

where a_i , b_i and c_i are empirical constants. The results show that the curves with the fixed exponent $c_i = 0.33$ provide the best fit for the dataset, which is in agreement with other studies (Wilson 2008; Moraes 2000; Businger et al. 1971).

In the above equation, u_* primarily occurs on both sides (in both definition of φ_i and ζ). According to insufficient independent scaling variables, construction of completely independent dimensionless groups and having no built-in correlation is inevitable (Andreas and Hicks 2002). Hence, self-correlation can lead to erroneous results in investigations using similarity theory (Klipp and Mahrt 2004). In spite of Baas et al. (2006) findings, as the other factors may attribute in the observed scatter in similarity functions more than self-correlation, this effect has been noted by others as “artificial, fictitious, or spurious correlation” (Grachev et al. 2007b). However, the mentioned dependency has been more pronounced for lower levels (2.2 and 3.2 m above ground) and under strong stable stratification (Grachev et al. 2007b; Sorbjan and Grachev 2010). For our analysis we would like to emphasize that we used data measured at the upper heights, and applied a method to reduce the averaging problems associated with self-correlation. Since a necessary condition for self-correlation is a large random scatter in data, thus reducing random scatter in data diminishes self-correlation (Grachev et al. 2012). Hence, using an independent bin-averaging method instead of conventional averaging reduces self-correlation effect (Grachev et al. 2007a). The success of this method has been proved by Grachev et al., (2008). To apply this method in the current work, at first the data were sorted for one parameter into bins. Then the local stability parameter has been averaged into bins with the width of 0.6. Afterward, mean and median values of $\langle u'w' \rangle$, $\langle v'w' \rangle$, $\langle w'T' \rangle$ and other relevant variables have been computed for each bin. Based on these averaged values, the stability parameter (1) and φ_i functions (2) have been computed for the local scaling. Furthermore, stability parameter has been plotted on the horizontal axis, based on the mean values, while the φ_i functions (using the Matlab' Curve Fitting Toolbox with 95 % confidence bounds) have been plotted on the vertical axis, based on the medians. To distinguish the effects of self-correlation, both results with and without self-correlation effects have been plotted in Fig. 6. For the

comparision purpose, the empirical constants for both methods have been listed in Table 3. Results demonstrate the decreased dependency on ζ values (through b_i values) and increase in a_i values for σ_u/u_{*l} and σ_v/u_{*l} , while no change occured for σ_w/u_{*l} values.

5.1.1 Longitudinal and lateral components of wind velocity

There are two schools of thought regarding application of non-dimensional standard deviations of horizontal components of wind velocity in unstable stratification. The first argues that these parameters do not follow MOST when normalized according to the rules of MOST (Panofsky et al. 1977); while the second group has shown that categorizing dataset according to wind speed (Martins et al. 2009) and stability parameter (Moraes et al. 2005), collapses non-dimensional parameters into similarity relations. Figure 6 illustrates the ζ dependence of σ_u/u_{*l} and σ_v/u_{*l} values achieved during the current work. Also our derived empirical constants from Eq. 1 have been listed in Table 3 alongside values from other studies for other surface types.

Empirical constants for Tehran, obtained from 105 m height, (2.69 for a_u ; Table 3) is greater than what has been reported in the literature. In addition, value of $b_u = 0.267$ (showing small dependence of σ_u/u_{*l} on ζ) is less than $b_u = 1.80, 2.01$ and 0.5 values, reported by Al-Jiboori et al. (2002) for Beijing, Xu et al. (1997) for Nanjing and Quan and Hu (2009) for Beijing, respectively, and shows more agreement with values obtained by Roth (2000) and Wood et al. (2010). Our proposed similarity relation for σ_v/u_{*l} has an empirical constant of $b_v = 0.146$ which is less than b_v values listed elsewhere and $a_v = 2.8$ that is greater than other findings for the other surface types (Table 3). Our proposed reasons for the almost twice value of b_v compared with the value of b_u may be due to (1) the mountains to the north that influence turbulent structure and decrease the dependency of σ_v/u_{*l} on ζ , and (2) enhanced turbulent transport of TKE out of the urban canopy as argued by Christen et al. (2009).

Our derived values for σ_u/u_{*l} and σ_v/u_{*l} are greater than those reported by Panofsky et al. (1977), who reached the expressions of $\sigma_{u,v}/u_{*l} = (12 + 0.5\zeta)^{0.33}$. Figure 6 also demonstrates the significant error introduced in prediction of turbulence intensities over Tehran, if similarity relations derived for the other locations be applied for Tehran. For example, application of Panofsky's relation at $\zeta = 10$ underestimates turbulence intensity in the u -component by 56 %, while Xu et al. (1997) similarity expression overestimates that by 20 %. The high degree of error strongly suggests that similarity relations for the fluctuations of

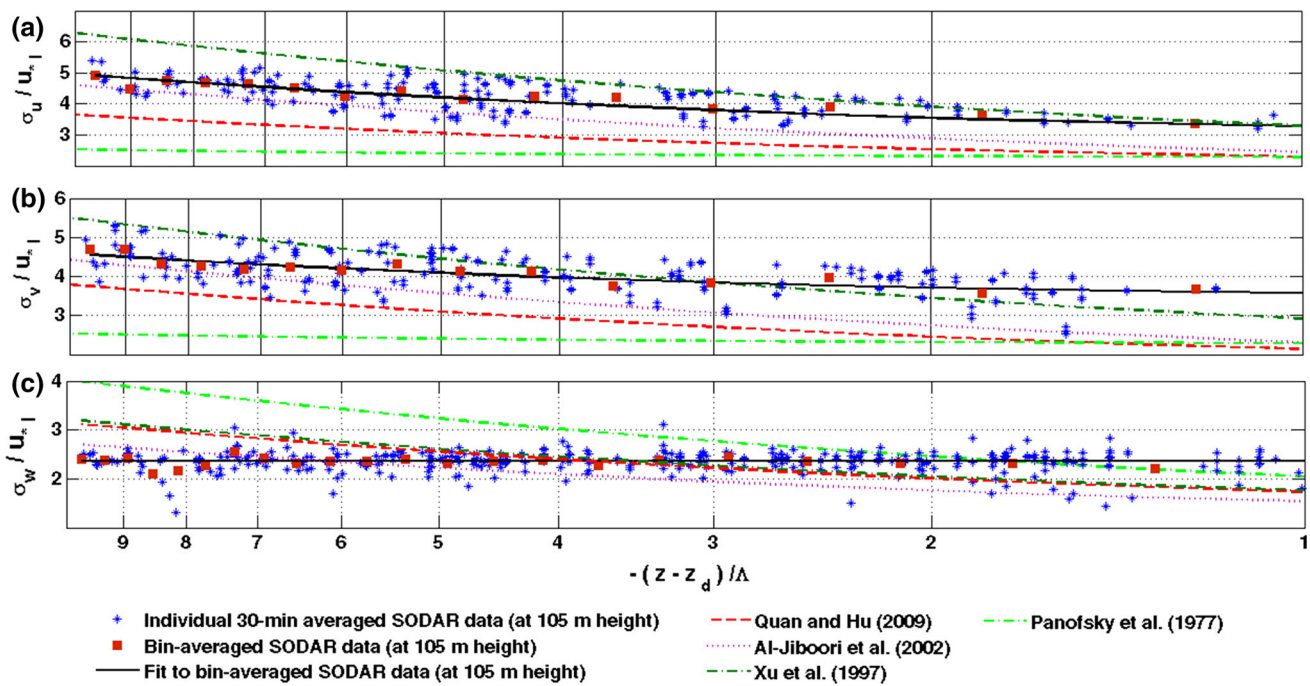


Fig. 6 Plots of non-dimensional turbulence intensity ($\varphi_i = \sigma_i/u_*$) for longitudinal (a), lateral (b) and vertical (c) components of wind velocity against ζ stability parameter in semi-log coordinates. Blue stars show individual 30-min averaged SODAR data (at 105 m height and normalized by local u_* , before self-correlation correction) and red squares represent bin-averaged SODAR data (at 105 m height and normalized by local u_* , after self-correlation correction), for Tehran dataset. The best-fitted trend to the bin-averaged SODAR data has

been also shown in thick solid lines (with 95 % confidence bounds), while results of prediction of other similarity functions obtained by Quan and Hu (2009), Al-Jiboori et al. (2002), Xu et al. (1997) and Panofsky et al. (1977) for Tehran data have been presented by dashed red lines, dotted pink lines, dashed-dotted dark green lines and dashed-dotted light green lines, respectively. Fitting has been done by least square analysis using Matlab® Curve Fitting Toolbox

horizontal components of wind velocity are unique to each terrain.

5.1.2 Vertical component of wind velocity

The dependence of σ_w/u_{*l} on ζ stability parameter, both calculated at 105 m height, has been plotted in Fig. 6c, while the derived empirical constants have been demonstrated in Table 3. The achieved value for a_w is greater than reported values elsewhere, similar to the values of a_u and a_v . The near zero dependence of σ_w/u_{*l} on ζ ($b_w = 0.0051$ in Table 3) for a wide range of unstable conditions (Fig. 6c) should be noted and is of significance. Our derived trend of σ_w/u_{*l} against the values of $-10 < \zeta < -1.7$ lies below the corresponding trend proposed by Panofsky et al. (1977) for rural area. This behaviour supports findings reported by Roth (1993) and Christen (2005, 2009) as the normalized vertical velocity standard deviation lies below that of rural surface layers. The constant value of σ_w/u_{*l} against ζ , calculated at 105 m height, implies that other forcings determine the vertical turbulence production over Tehran. The near zero dependency of σ_w/u_{*l} on ζ justifies the essence of further research using other scaling parameters.

5.2 Non-dimensional standard deviations of wind velocity components, using w_* and z_i scales

Numerous studies have shown that large convective motions which span the entire depth of the atmospheric boundary-layer influence wind velocity variances all the way to the surface. These large-scale motions, which are influenced by outer-layer (out of surface layer) and obey its scales (Eting and Brown 1993), interact with the small-scale turbulence that obeys inner surface-layer scaling (Adrian et al. 2000). Castillo et al. (2011) suggested that there is a significant interaction between the outer-layer horizontal and inner surface-layer vertical motions which influences surface-layer fluxes. In addition, strong vertical mixing in unstable stratification produces vigorous turbulence that justifies the need for a more comprehensive scale (Roth 1993; Panofsky et al. 1977; Moraes et al. 2005). To investigate the applicability of this idea for Tehran, $w_* = (gz_i w' \theta'/T_0)^{1/3}$ convective velocity scale was used (Table 2, 6th row). This velocity scale and also the stability parameter of $(z - z_d)/z_i$ is closely related to z_i length scale. Hereby, the properties of z_i has been examined to reveal whether or not it depicts a more accurate description of the turbulence behaviour. Results of the evaluation of similarity theory using z_i and w_*

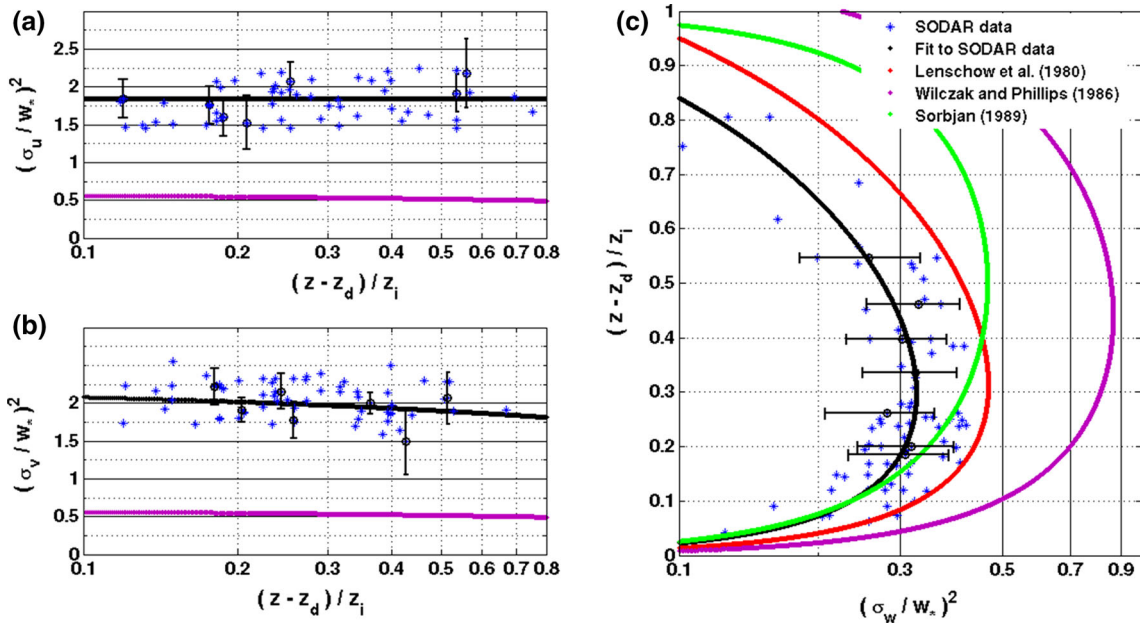


Fig. 7 Non-dimensional standard deviation of along-wind (**a**), cross-wind (**b**) and vertical (**c**) components of wind velocity (form SODAR data at 105 m height) scaled by w_* , against the stability parameter of $(z - z_d)/z_i$. Also to highlight the dependency between $(\sigma_w/w_*)^2$ and $(z - z_d)/z_i$, results were depicted by converting axes location ($x \rightarrow y$), compare with subplots (**a**) and (**b**). SODAR results are depicted as

scales for σ_u , σ_v and σ_w parameters at 105 m height of our dataset have been discussed below.

5.2.1 u - and v -components of wind velocity

To investigation the dependency of σ_u/w_* and σ_v/w_* values (measured numerators and calculated denominators, all at 105 m height) on $(z - z_d)/z_i$, a relation in the form of $(\frac{\sigma_u}{w_*})^2 = m_1(m_2((z - z_d)/z_i)^{1/2}) + m_4((z - z_d)/z_i)^{1/2})^n$ has been fitted to the calculated parameters. This relationship is similar to the formulation introduced by Wilczak and Phillips (Wilczak and Phillips 1986) with the exponent of $n = 1/2$ and constants of 0.74, 0.5, 2 and 0.3 for $m_{1,2,3,4}$, respectively. Our obtained empirical similarity expressions for σ_u/w_* and σ_v/w_* have been shown below as:

$$\left(\frac{\sigma_u}{w_*}\right)^2 = 0.67 \left(2.29 \left(1.2 - \left(\frac{z - z_d}{z_i} \right)^{\frac{1}{2}} \right) + 2.29 \left(\frac{z - z_d}{z_i} \right)^{\frac{1}{2}} \right)^1 \quad (2)$$

and

$$\left(\frac{\sigma_v}{w_*}\right)^2 = 1.0 \left(1.71 \left(1.3 - \left(\frac{z - z_d}{z_i} \right)^{\frac{1}{2}} \right) + 1.25 \left(\frac{z - z_d}{z_i} \right)^{\frac{1}{2}} \right)^1. \quad (3)$$

stars. Black solid lines were fitted to SODAR data with 95 % confidence bounds using Matlab' Curve Fitting Toolbox. Also vertical error bars (in **a** and **b** subplots) and horizontal error bar (in **c** subplot) have been added for seven random data, to avoid the crowded plots

These similarity expressions, shown in Fig. 7a, b, indicate that the obtained empirical constants for turbulent intensity for u - and v -components are different that highlights the anisotropic nature of the turbulence in this area, emphasized by Pegahfar et al. (2011). Findings of the current work show that non-isotropic feature of turbulence structure has been emerged in horizontal direction that supports the results obtained by Bredberg (2002) and Wu et al. (2004).

It is important to note that $(\sigma_u/w_*)^2$ and $(\sigma_v/w_*)^2$ obtained from our dataset are significantly different than the results reported for the other cities (Wood et al. 2010 for London City, their Fig. 8). This difference is noticeable for $(z - z_d)/z_i$ values greater than 0.15. In addition $(\sigma_u/w_*)^2$ and $(\sigma_v/w_*)^2$ values are typically greater than 1, while Wilczak and Phillips (1986) obtained the values of 1 for both $(\sigma_u/w_*)^2$ and $(\sigma_v/w_*)^2$, as well as Wood et al. (2010) reached the value of 0.5 (for more details see Fig. 8 in Wood et al. 2010). Additionally, the complex form of Eq. 2 has been fitted to our dataset for a comparison purpose with other results reported in the literature for other surface types. However, the relatively constant trends with the value of around 2 for both parameters of $(\sigma_u/w_*)^2$ and $(\sigma_v/w_*)^2$ with slow variation against $(z - z_d)/z_i$ values have been achieved as “ $\sigma_{u,v}/w_* = 0.06((z - z_d)/z_i) + 1.92$ ” for the current cases.

Table 4 List of empirical constants derived from fitting Eq. 4, using Tehran dataset and also from some other research studies

Author	Comments (z_d)	m_1	n_1	m_2	n_2
This study	12	1.3	2/3	0.84	2
Lenschow et al. (1980)	0.0	1.8	2/3	0.8	2
Sorbjan (1989)	0.0	1.17	2/3	1	2/3
Wilczak and Phillips (1986)	0.0	2.5	2/3	0.91	1/2

5.2.2 Vertical component of wind velocity

To fit similarity expression for $(\sigma_w/w_*)^2$ (calculated at 105 m height), the expression of

$$\left(\frac{\sigma_w}{w_*}\right)^2 = m_1 \left(\frac{z - z_d}{z_i}\right)^{n_1} \left(1 - m_2 \left(\frac{z - z_d}{z_i}\right)\right)^{n_2}, \quad (4)$$

has been implemented, based on the widely accepted idealized profile of Lenschow et al. (1980). Using the Matlab Curve Fitting Toolbox, our obtained similarity relation is:

$$\begin{aligned} \left(\frac{\sigma_w}{w_*}\right)^2 &= 1.3 \left(\frac{z - z_d}{z_i}\right)^{2/3} \left(1 - 0.84 \left(\frac{z - z_d}{z_i}\right)^1\right) \\ &\times \left(1 - 0.84 \left(\frac{z - z_d}{z_i}\right)^1\right). \end{aligned} \quad (5)$$

Results of the empirical constants from the present work are listed in Table 4, alongside available values in the literature; the proposed curves are illustrated in Fig. 7c. Calculated values of $(z - z_d)/z_i$ have a maximum value of 0.45 for Tehran and do not reach the value of 1. The ratio of $(z - z_d)/z_i$ is small due to the large values attained by z_i , with monthly average values that varied from 247 m for winter and autumn months to 3000 m for summer and spring ones over Tehran (Pegahfar et al. 2013; Ahmadi-Givi et al. 2008). Overall, change of scaling parameters leads to more reliable similarity function for $(\sigma_w/w_*)^2$. This may be attributed to the local-free convection effects that have been indirectly considered in w_* and z_i scales.

6 Conclusions

This paper presented an analysis of the validity and limitation of the similarity theory for the normalized fluctuations of wind velocity under unstable conditions for Tehran, an urban area located in a complex mountainous terrain.

Using data from a SODAR and five 2-D sonic anemometers, of which four had been installed on a 100-m tower, illustrated that MOST could not be applied for the data measured at the heights lower than 105 m (e.g. 45 and 75 m height). At 105 m height, turbulent intensities could be matched in similarity theory using two groups of scales:

1. u_* and Λ : After self-correlation correction, the similarity expressions with the fixed exponent of 0.33 for the calculated values of φ_u , φ_v and φ_w have been proposed for Tehran. The empirical fits for the horizontal components followed well and showed a general increase with increasing instability. However, our obtained functions for φ_u , φ_v and φ_w differ from the ones reported in the other studies from the other locations. So it can be clearly inferred that using the known similarity relations produced noticeable underestimation or overestimation in prediction of turbulent intensities for Tehran and the discrepancy for the vertical component is even more acute. One of the remarkable points arrived in the current work is the near zero slope between σ_w/u_{*l} and ζ , which may be due to the dominance of some unknown local forcings.

2. w_* and z_i : Our results demonstrate that these scales provide appropriate similarity expressions. Our achieved similarity expressions of σ_u/w_* and σ_v/w_* show similar behaviour with small difference only for individual empirical parameters maybe due to the non-homogenous characteristics of the local terrain. Hence, a reasonable match for both of σ_u/w_* and σ_v/w_* have been achieved with one single mathematical relationship with small dependency on stability parameter. Moreover, these scalings also produce better results for σ_w/w_* , as compared to ζ stability parameter, indicating that turbulent structure over Tehran are influenced by the large and convectively driven eddies (i.e. the velocity and length scales of these eddies contribute to turbulence intensities).

Further, it is shown that (a) the dimensionless standard deviations of wind velocity over Tehran could be collapsed into similarity functions including empirical constants that demonstrate considerable difference with those suggested in the literature, due to the unique characteristics of the physical setting, (b) localized influence of interaction between inner- and outer-layer turbulence structure (using two groups of scales for velocity and length, belonging to the inner- and outer- layer) over Tehran is not as significant as local forcing effects, in agreement with findings of Castillo et al. (2011) who argued that the interaction between outer- and inner-layer may be negligible, and (c) the applicability of “transformation from one kind of similarity scale to another one”, as proposed by Hu and Zhang (1993) is dependent on the chosen variable and its vertical location. In the current work, the hypothesis

suggested by Hu and Zhang (1993), who used data from a 213-m tower in Tsukuba Science city in Japan and verified local similarity relations for various similarity scales, acts well for φ_u and φ_v , but not for φ_w . Hopefully our findings can be applied in numerical simulation over the selected area.

Acknowledgments The authors would like to thank the joint effort of all members of Institute of Geophysics of University of Tehran for providing SODAR and tower data and also Iranian National Institute for Oceanography and Atmospheric Science. The authors acknowledge M.M. Farahani for his crucial collaboration in data collection and handling.

References

- Adrian RJ (2002) Information and the study of turbulence and complex flow. *JSME J Ser B* 45:2–8
- Adrian RJ, Meinhart CD, Tomkins CD (2000) Vortex organization in the outer region of the turbulent boundary layer. *J Fluid Mech* 422:1–53
- Ahmadi-Givi F, Sabetghadam S, Aliakbari-Bidokhti AA (2008) Studying the fluctuation of mixed layer height of Tehran, using MM5 modeling system. *Journal of Earth and Space Physics* 35:105–117
- Al-Jiboori M (2008) Correlation coefficients in urban turbulence. *Boundary-Layer Meteorol* 126:311–323
- Al-Jiboori M, Xu Y, Qian Y (2002) Local similarity relationships in the urban boundary layer. *Boundary-Layer Meteorol* 102:63–82
- Andreas EL, Hicks BB, (2002) Comments on “Critical test of the validity of Monin–Obukhov similarity during convective conditions.” *J Atmos Sci* 59:2605–2607
- Anfossi D, Oettl D, Degrazia G, Boulart A (2005) An analysis of sonic anemometer observations in low wind speed conditions. *Boundary-Layer Meteorol* 114:179–203
- Arya SPS (1981) Parameterizing the height of the stable atmospheric boundary layer. *J Appl Meteor* 20:1192–1202
- Asanuma J, Brutsaert W (1999) The effect of chessboard variability of the surface fluxes on the aggregated turbulence fields in a convective atmospheric surface layer. *Boundary-Layer Meteorol* 91(1):37–50
- Baas P, Steeneveld GJ, Van De Wiel BJH, Holtslag AAM (2006) Exploring self-correlation in flux-gradient relationships for stably stratified conditions. *J Atmos Sci* 63(11):3045–3054
- Bou-Zeid E, Overney J, Rogers B, Parlange M (2009) The effects of building representation and clustering in large eddy simulations of flows in urban canopies. *Boundary-Layer Meteorol* 132:415–436
- Bredberg J (2002) Turbulence Modelling for Internal Cooling of Gas-Turbine Blades. PhD thesis, Chalmers University Of Technology GO Teborg, Sweden
- Britter R, Hanna S (2003) Flow and dispersion in urban areas. *Annu Rev Fluid Mech* 35:469–496
- Businger J, Wyngaard J, Izumi Y, Bradley E (1971) Flux profile relationship in the atmospheric surface layer. *J Atmos Sci* 28:181–189
- Castillo MC, Inagaki A, Kanda M (2011) The Effects of inner- and outer-layer turbulence in a convective boundary layer on the near-neutral inertial sublayer over an urban-like surface. *Boundary-Layer Meteorol* 140:453–469
- Cava D, Giostra U, Siqueira M, Katul GG (2004) Organized motion and radiative perturbations in the nocturnal canopy sublayer above an even-aged pine forest. *Boundary-Layer Meteorol* 112(1):129–157
- Christen A (2005) Atmospheric turbulence and surface energy exchange in urban environments. Results from the Basel Urban Boundary Layer Experiment (BUBBLE), Vol 11 of Stratus, ISBN 3-85977-266-X
- Christen A, Vogt R (2004) energy and radiation balance of a central European city. *Int J Climatol* 24:1395–1421
- Christen A, Rotach MW, Vogt R (2009) The Budget of Turbulent Kinetic Energy in the Urban Roughness Sublayer. *Boundary-Layer Meteorol* 131:193–222
- Cvitanc L (2006) Classification of the stratified atmospheric boundary layers at Molive (Croatia) based on the similarity theory. *Meteorol Atmos Phys* 93:235–246
- Detto M, Baldocchi D, Katul GG (2010) Scaling properties of biologically active scalar concentration fluctuations in the atmospheric surface layer over a managed Peatland. *Boundary-Layer Meteorol* 136:407–430
- Etling D, Brown RA (1993) Roll vortices in the planetary boundary layer: a review. *Boundary-Layer Meteorol* 65:215–248
- Feigenwinter C, Vogt R (2005) Detection and analysis of coherent structures in urban turbulence. *Theor Appl Climatol* 81:219–230
- Feigenwinter C, Vogt R, Parlow E (1999) Vertical structure of selected turbulence characteristics above an urban canopy. *Theor Appl Climatol* 62:51–63
- Finnigan JJ, Einaudi F, Fua D (1984) The interaction between an internal gravity-wave and turbulence in the stably-stratified nocturnal boundary-layer. *J Atmos Sci* 41(16):2409–2436
- Garratt JR (1982) Observations in the nocturnal boundary layer. *Boundary-Layer Meteorol* 22:21–48
- Gaynor SE, Kristensen L (1986) Errors in second moments estimated from monostatic Doppler sodar winds. Part II: application to field measurements. *J Atmos Ocean Technol* 3(3):529–534
- Grachev AA, Fairall CW, Persson POG, Andreas EL, Guest PS (2005) Stable boundary-layer scaling regimes: the SHEBA data. *Boundary-Layer Meteorol* 116:201–235
- Grachev AA, Andreas EL, Fairall CW, Guest PS, Persson POG (2007a) SHEBA flux-profile relationships in the stable atmospheric boundary layer. *Boundary-Layer Meteorol* 124:315–333
- Grachev AA, Andreas EL, Fairall CW, Guest PS, Persson POG (2007b) On the turbulent Prandtl number in the stable atmospheric boundary layer. *Boundary-Layer Meteorol* 125(2):329–341
- Grachev AA, Andreas EL, Fairall CW, Guest PS, Persson POG (2008) Turbulent measurements in the stable atmospheric boundary layer during SHEBA: ten years after. *Acta Geophys* 56(1):142–166
- Grachev AA, Andreas EL, Fairall CW, Guest PS, Persson POG (2012) Outlier problem in evaluating similarity functions in the stable atmospheric boundary layer. *Boundary-Layer Meteorol* 144(2):137–155
- Grachev AA, Andreas EL, Fairall CW, Guest PS, Persson POG (2015) Similarity theory based on the Dougherty–Ozmidov length scale. *Quarterly Journal of the Royal Meteorological Society* 141(690):1845–1856
- Hagishima A, Tanimoto J, Nagayama K, Meno S (2009) Aerodynamic parameters of regular arrays of rectangular blocks with various geometries. *Boundary-Layer Meteorol* 132:315–337
- Hanna S, White J, Zhou Y (2007) Observed winds, turbulence and dispersion in built-up downtown areas in Oklahoma City and Manhattan. *Boundary-Layer Meteorol* 125:441–468
- Hu Y, Zhang Q (1993) On local similarity of the atmospheric boundary layer. *Sci Atmosph Sin* 17:10–20
- Inagaki A, Kanda M (2008) Turbulent flow similarity over an array of cubes in near-neutrally stratified atmospheric flow. *J Fluid Mech* 615:101–120

- Inagaki A, Kanda M (2010) Organized structure of active turbulence over an array of cubes within the logarithmic layer of atmospheric flow. *Boundary-Layer Meteorol* 135:209–228
- Ito Y (1997) Errors in wind measurements estimated by five-beam phased array Doppler sodar. *Journal of Atmospheric and Oceanic Technology* 14(4):792–801
- Kaimal J (1978) Horizontal velocity spectra in an unstable surface layer. *J Atmos Sci* 35:18–24
- Katul GG, Goltz SM, Hsieh CI, Cheng Y, Mowry F, Sigmon J (1995) Estimation of surface heat and momentum fluxes using the flux-variance method above uniform and non-uniform terrain. *Boundary-Layer Meteorol* 74(3):237–260
- Klipp CL, Mahrt L (2004) Flux-gradient relationship, self-correlation and intermittency in the stable boundary layer. *Quart J Roy Meteorol Soc* 130(601):2087–2103
- Kouznetsov R, Kramar VF, Kalistratova MA (2007) The vertical structure of turbulent momentum flux in the lower part of the atmospheric boundary layer. *Meteorol Z* 16(4):367–373
- Krishnan P, Kunhikrishnan PK (2002) Some characteristics of atmospheric surface layer over a tropical inland region during southwest monsoon period. *Atmos Res* 62:111–124
- Lamaud E, Irvine M (2006) Temperature and humidity dissimilarity and heat-to-water-vapour transport efficiency above and within a pine forest canopy: the role of the Bowen ratio. *Boundary-Layer Meteorol* 120(1):87–109
- Laubach J, McNaughton KG (2009) Scaling properties of temperature spectra and heat-flux cospectra in the surface friction layer beneath an unstable outer layer. *Boundary-Layer Meteorol* 133:219–252
- Lenschow DH, Wyngaard JC, Pennell WT (1980) Mean-field and second moment budgets in a baroclinic, convective boundary layer. *J Atmos Sci* 37:1313–1326
- Liu X, Ohtaki E (1997) An independent method to determine the height of the mixed layer. *Boundary-Layer Meteorol* 85:497–504
- Mahrt L (1998a) Flux sampling errors for aircraft and towers. *J Atmos Oceanic Tech* 15:416–429
- Mahrt L (1998b) Stratified atmospheric boundary layers and breakdown of models. *Theoret Comput Fluid Dyn* 11:263–279
- Martins CA, Moraes OLL, Acevedo OC, Degrazia GA (2009) Turbulence intensity parameters over a very complex terrain. *Boundary-Layer Meteorol* 133:35–45
- McNaughton KG, Laubach J (1998) Unsteadiness as a cause of non-equality of eddy diffusivities for heat and vapour at the base of an advective inversion. *Boundary-Layer Meteorol* 88(3):479–504
- Melas D (1991) Using a simple resistance law to estimate friction velocity from SODAR measurements (research note). *Boundary-Layer Meteorol* 57:275–287
- Monin AS, Obukhov AM (1954) Main characteristics of the turbulent mixing in the atmospheric surface layer. *Trudy Geophys Inst AN SSSR* 24:153–187
- Moraes OLL (2000) Turbulence characteristics in the surface boundary layer over the South American pampa. *Boundary-Layer Meteorol* 96:317–335
- Moraes OLL, Acevedo OC, Degrazia GA, Anfossi D, da Silva R, Anabor V (2005) Surface layer turbulence parameters over complex terrain. *Atmos Environ* 39:3103–3112
- Moriwaki R, Kanda M (2006) Flux-gradient profiles for momentum and heat over an urban surface. *Theor Appl Climatol* 84:127–135
- Moriwaki R, Kanda M, Watanabe T (2002) Turbulent transfer efficiency of momentum, heat, vapor, and CO₂ measured in the urban surface layer over a densely built-up canopy. Preprints. In 15th Symposium on Boundary Layers and Turbulence, American Meteorological Society, Wageningen, The Netherlands, July 2002
- Mortarini L, Ferrero E, Richiardone R, Falabino S, Anfossi D, TriniCastelli S, Carretto E (2009) Assessment of dispersion parameterizations through wind data measured by three sonic anemometers in a urban canopy. *Adv Sci Res* 3:91–98
- Murty KPRV, Prasad GSSD, Sa LDA, Filho EPM, de Souza A, Malhi Y (1998) A method to determine the height of the mixed layer from spectral peak frequency of horizontal velocity. In: X Congresso Brasileiro de Meteorologia, Brasília. Anais do X Congresso Brasileiro de Meteorologia, 4 pp
- Nakamura Y, Oke TR (1988) Wind, temperature and stability conditions in an east-west oriented urban canyon. *Atmos Environ* 22(12):2691–2700
- Nieuwstadt F (1984) The turbulent structure of the stable nocturnal boundary layer. *J Atmos Sci* 41:2202–2216
- Pahlow M, Parlange M, Prête-Agél F (2001) On Monin-Obukhov similarity in the stable atmospheric boundary layer. *Boundary-Layer Meteorol* 99:225–247
- Panofsky HA, Tennekes H, Lenschow DH, Wyngaard JC (1977) The characteristics of turbulent velocity component in the surface layer under convective conditions. *Boundary-Layer Meteorol* 11:355–361
- Pegahfar N, Bidokhti AA (2013) Similarity relations in a stable and relatively neutral surface layer in an urban area with complex topography (Tehran). *Environ Fluid Mech* 13:1–31
- Pegahfar N, Bidokhti AA, Zawar-Reza P, Farahani MM (2011) Study of vertical wind profiles in an urban area with complex topography (Tehran). *J Earth Syst Sci* 120(5):825–841
- Pegahfar N, Bidokhti AA, Zawar-Reza P (2013) Parameterization of Nocturnal Stable Boundary Layer Height (NSBLH) and effect of NSBLH on air pollution in an urban area with complex topography (Tehran). *Journal of the Earth and Space Physics* 38(2):1–15
- Petenko I, Mastrantonio G, Viola A, Argentini S, Pietroni I (2012) Wavy Vertical Motions in the ABL Observed by Sodar. *Boundary-Layer Meteorol* 143:125–141
- Prabha TV, Leclerc MY, Karipot A, Hollinger DY (2007) Low-frequency effects on eddy covariance fluxes under the influence of a low-level jet. *J Appl Meteorol Climatol* 46(3):338–352
- Princevac M, Venkatram A (2007) Estimating micrometeorological inputs for modeling dispersion in urban areas during stable conditions. *Atmos Environ* 41:5345–5356
- Quan L, Hu F (2009) Relationship between turbulent flux and variance in the urban canopy. *Meteorol Atmos Phys* 104:29–36
- Rotach MW (1993a) Turbulence close to a rough urban surface, Part I: Reynolds stress. *Boundary-Layer Meteorol* 65:1–28
- Rotach MW (1993b) Turbulence close to a rough urban surface, Part II: variances and gradients. *Boundary-Layer Meteorol* 66:75–92
- Roth M (1993) Turbulent transfer relationships over an urban surface II: integral statistics. *Q J R Meteorol Soc* 119:1105–1120
- Roth M (2000) Review of atmospheric turbulence over cities. *Q J R Meteorol Soc* 126:941–990
- Roth M, Salmond JA, Satyanarayana ANV (2006) Methodological consideration regarding the measurements of turbulent fluxes in the urban roughness sublayer: the roll of scintillometry. *Boundary-Layer Meteorol* 121:351–375
- Seibert P, Langer M (1996) Deriving characteristic parameters of the convective boundary layer from SODAR measurements of the vertical velocity variance. *Boundary-Layer Meteorol* 81:1–22
- Sorbian Z (1989) Structure of the atmospheric boundary layer. Prentice-Hall INC, New Jersey, p 317
- Sorbian Z, Grachev AA (2010) An evaluation of the flux-gradient relationship in the stable boundary layer. *Boundary-Layer Meteorol* 135(3):385–405
- Stull R (1988) An introduction to boundary layer meteorology. Kluwer Academic Publishers, Dordrecht, p 666

- Thomas R, Vogt S (1993) Inter-comparison of turbulence data measured by SODAR and sonic anemometers. *Boundary-Layer Meteorol* 62:353–359
- Weber S, Kordowski K (2010) Comparison of atmospheric turbulence characteristics and turbulent fluxes from two urban sites in Essen, Germany. *Theor Appl Climatol* 102:61–74
- Wilczak JM, Phillips MS (1986) An indirect estimation of convective boundary layer structure for use in pollutant dispersion models. *J Clim Appl Meteorol* 25:1609–1624
- Wilson JD (2008) Monin-Obukhov functions for standard deviations of velocity. *Boundary-Layer Meteorol* 129:353–369
- Wood CR, Lacser A, Barlow JF, Padhra A, Belcher SE, Nemitz E, Helfter C, Famulari D, Grimmond CSB (2010) Turbulent flow at 190 m height above London during 2006–2008: a climatology and the applicability of similarity theory. *Boundary-Layer Meteorol* 137:77–96
- Wu W, Wang P, Chiba N (2004) Comparison of Five depth-averaged 2-D turbulence models for river flows. *Archives Hydro-Eng Environ Mech* 51(2):183–200
- Wyngaard JC, Cote OR (1971) The budget of turbulent kinetic energy and temperature variance in the atmospheric surface layer. *J Atmos Sci* 28:190–201
- Xu Y, Zhou C, Li Z et al (1997) Turbulent structure and local similarity in the tower-layer over the Nanjing area. *Boundary-Layer Meteorol* 82:1–21
- Yusup Y, Lim JF (2012) Turbulence variances in the convective urban roughness sublayer: an application of similarity theory using local scales. *Meteorol Appl*. doi:[10.1002/met.1316](https://doi.org/10.1002/met.1316)
- Zawar-Reza P, Appelhans T, Gharaylou M, Shamsipour A (2010) Mesoscale control for mega city in a semi-arid mountainous environment: tehran, Iran. *Int J Environ Pollut* 41:166–183